

CRITICAL PROBLEMS OF BOUSSINESQ-TYPE TURBULENCE MODEL APPLICATION IN INTERNAL COMBUSTION ENGINES

Oldřich Vítek*, Miloš Polášek†, Karel Kozel‡, Jan Macek§

Czech Technical University in Prague, Josef Božek Research Center, Prague

Abstract

The presented paper deals with discussion of weak points when Boussinesq-type turbulence models are applied for modelling phenomena in ICE. The following are the important problematic factors – turbulence momentum transport, dissipation equation, modelling of SI engine combustion. Examples are presented. The contribution is just stating some facts, no general conclusions how to solve the mentioned problematic cases are presented.

1 Introduction

Nowadays it is a usual routine to apply two-equation turbulence models for modelling of compressible transient turbulent flow in internal combustion engine (ICE). No special turbulence models for ICE are developed. Instead, classical models (developed for the needs of external aerodynamics) are applied (the model constants might be slightly different). The exception might be a three-equation turbulence model of the company *AVL Graz*, the model is labelled $k - \zeta - f$ and is applied in their CFD code FIRE [1]. There is really a large amount of papers where results of such simulations are presented including comparison with experimental data. What is missing (or it is unknown to the authors) is that no comprehensive comparison of measured Reynolds stresses with predicted/calculated ones is carried out (the authors are aware of the fact that it is not easy to measure Reynolds stress tensor components in ICE under typical operating conditions). It is a critical question as correlations of fluctuating terms of Favre averaged mathematical model (equations 1, 2 and 3) are the dominant ones in ICE. If there is not good correspondence with momentum turbulent transport, internal energy (temperature) turbulent transport cannot be trusted either. This would have significant consequences for all the calculations based on chemical kinetics as these computations are very sensitive to local temperature. When working on [14], these problems arisen again. The presented paper main target is to stress some problems of turbulence modelling based on Boussinesq hypothesis for the case of ICE.

*Ing., Ph.D., e-mail: Oldrich.Vitek@fs.cvut.cz

†Doc. Ing., Ph.D., e-mail: Milos.Polasek@fs.cvut.cz

‡Prof. RNDr., DrSc., e-mail: Karel.Kozel@fs.cvut.cz

§Prof. Ing., DrSc., e-mail: Jan.Macek@fs.cvut.cz

2 Theoretical Background

In this section, a brief description of the applied mathematical model is presented. A more detailed description of the whole mathematical model can be found in [14, 19]. The mathematical model is based on a Favre-averaged integral Navier-Stokes equation set written for arbitrary movable control volume (Advanced Multizone Eulerian Model) – equations (1), (2) and (3) plus additional relations (4) - (13). Favre decomposition is defined through equations (4)-(9).

$$\frac{d}{dt} \int_{V_{ib}} \bar{\rho} dV = - \int_{\partial V_{ib}} \bar{\rho} (\tilde{w}_j - w_{Gj}) n_j dS \quad (1)$$

$$\begin{aligned} \frac{d}{dt} \int_{V_{ib}} \bar{\rho} \tilde{w}_i dV = & - \int_{\partial V_{ib}} \bar{\rho} \tilde{w}_i (\tilde{w}_j - w_{Gj}) n_j dS + \int_{V_{ib}} \bar{\rho} g_i dV \\ & + \int_{\partial V_{ib}} \left[-\bar{p} \delta_{ij} + \bar{\tau}_{ij} + \left(-\overline{\rho w_i'' w_j''} \right) \right] n_j dS \end{aligned} \quad (2)$$

$$\begin{aligned} \frac{d}{dt} \int_{V_{ib}} \bar{\rho} \tilde{e} dV = & - \int_{\partial V_{ib}} \bar{\rho} \tilde{e} (\tilde{w}_j - w_{Gj}) n_j dS + \int_{V_{ib}} \bar{\rho} g_j \tilde{w}_j dV \\ & + \int_{\partial V_{ib}} \left[-\bar{p} \delta_{ij} + \bar{\tau}_{ij} + \left(-\overline{\rho w_i'' w_j''} \right) \right] \tilde{w}_i n_j dS \\ & + \int_{\partial V_{ib}} \left(\bar{\tau}_{ij} w_i'' - \frac{1}{2} \overline{\rho w_j'' w_i'' w_i''} \right) n_j dS \\ & - \int_{\partial V_{ib}} \left[\bar{q}_j + \left(\overline{\rho w_j'' u''} + \overline{p \delta_{ij} w_i''} \right) \right] n_j dS \\ & + \int_{V_{ib}} \bar{Q}_V dV \end{aligned} \quad (3)$$

$$\rho = \bar{\rho} + \rho' \quad (4)$$

$$p = \bar{p} + p' \quad (5)$$

$$w_i = \tilde{w}_i + w_i'' \quad (6)$$

$$u = \tilde{u} + u'' \quad (7)$$

$$T = \tilde{T} + T'' \quad (8)$$

$$\bar{\rho} \tilde{e} \equiv \bar{\rho} \tilde{e} = \bar{\rho} \tilde{u} + \bar{\rho} \frac{\tilde{w}_i \tilde{w}_i}{2} + \frac{\overline{\rho w_i'' w_i''}}{2} + \bar{\rho} \psi \quad (9)$$

$$\bar{p}V = \bar{m}r\tilde{T} \quad (10)$$

$$\tilde{u} = \tilde{u}_0 + \overline{c_v(\tilde{T})}_{T_{ref}} (\tilde{T} - T_{ref}) \quad (11)$$

$$\bar{\tau}_{ij} = \mu(\tilde{T}) \left(\frac{\partial \tilde{w}_i}{\partial x_j} + \frac{\partial \tilde{w}_j}{\partial x_i} \right) + \left(\lambda_S - \frac{2}{3} \mu(\tilde{T}) \right) \frac{\partial \tilde{w}_k}{\partial x_k} \delta_{ij} \quad (12)$$

$$\bar{q}_i = -\lambda(\tilde{T}) \frac{\partial \tilde{T}}{\partial x_i} \quad (13)$$

Boussinesq hypothesis (14) is applied for modelling of momentum turbulent transport term – algebraic, one- and two-equation turbulence models are used, the exact model definition can be found in [14, 21]. The turbulence modelling theory is based mainly on [21], the remaining fluctuating correlations are model by means of equations (15)-(16).

$$\bar{S}_{ij} \equiv \frac{1}{2} \left(\frac{\partial \tilde{w}_i}{\partial x_j} + \frac{\partial \tilde{w}_j}{\partial x_i} \right) \quad (14a)$$

$$\tau_{ij}^R \equiv -\overline{\rho w_i'' w_j''} = 2\mu_T \left(\bar{S}_{ij} - \frac{1}{3} \frac{\partial \tilde{w}_k}{\partial x_k} \delta_{ij} \right) - \frac{2}{3} \bar{\rho} k \delta_{ij} \quad (14b)$$

$$\dot{q}_{turb,i} \equiv \overline{\rho w_i'' u''} + \overline{p \delta_{ji} w_j''} = -\frac{\mu_T (c_v(\tilde{T}) + r)}{Pr_T} \frac{\partial \tilde{T}}{\partial x_i} \quad (15)$$

$$\overline{w_j'' w_i''} + \left(-\frac{1}{2} \overline{\rho w_j'' w_i'' w_i''} \right) = \left(\mu + \frac{\mu_T}{\sigma_k} \right) \frac{\partial k}{\partial x_j} \quad (16)$$

From numerical point of view, the finite volume cell-centered method is implemented. The numerical solution is performed by means of explicit multi-stage Runge-Kutta method (e.g. [5, 13]).

As far as modelling of combustion is concerned, the *Level Set* approach is applied – equations (17)-(18). Arbitrary function (\tilde{G}) transport is used to model flame front propagation in the space domain – more detailed description can be found in [10, 11]. Mass balance of each considered component (air, fuel and burnt gas) is written in equation set (19), diffusion across the flame front is neglected. Source term in energy equation due to combustion process is defined in Equation (20). The combustion in each finite volume is modelled by means of constant rate-of-heat-release (ROHR) depending only on the amount of combustible mixture in a finite volume and combustion duration being function of size of the finite volume only. The ROHR is labelled as x function in presented equations. Combustion itself is started when prescribed level of the arbitrary function \tilde{G} is reached in the finite volume.

$$\frac{d}{dt} \int_{V_{ib}} \bar{\rho} \tilde{G} dV = - \int_{\partial V_{ib}} \bar{\rho} \tilde{G} (w_j - w_{Gj}) n_j dS + \int_{\partial V_{ib}} \frac{\bar{\rho} s_T^0 \tilde{G}}{\left(\frac{\partial \tilde{G}}{\partial x_j} \frac{\partial \tilde{G}}{\partial x_j} \right)^{\frac{1}{2}}} \frac{\partial \tilde{G}}{\partial x_i} n_i dS \quad (17)$$

$$\frac{s_T^0}{s_L^0} = 1 + C_1 \left(\frac{w'}{s_L^0} \right)^n \quad (18a)$$

$$s_L^0 = f(p, T, \lambda) \quad (18b)$$

$$w' \approx w_i'' = \sqrt{\frac{2}{3} k} \quad (18c)$$

$$\frac{d}{dt} \int_{V_{iib}} \bar{\rho}_{pal} dV = - \int_{\partial V_{iib}} \bar{\rho}_{pal} (\tilde{w}_j - w_{Gj}) n_j dS - \frac{\int_{V_{iib}} \bar{\rho}_{pal} dV}{1-x} \frac{dx}{dt} \quad (19a)$$

$$\frac{d}{dt} \int_{V_{iib}} \bar{\rho}_{vzd} dV = - \int_{\partial V_{iib}} \bar{\rho}_{vzd} (\tilde{w}_j - w_{Gj}) n_j dS - L_T \frac{\int_{V_{iib}} \bar{\rho}_{pal} dV}{1-x} \frac{dx}{dt} \quad (19b)$$

$$\frac{d}{dt} \int_{V_{iib}} \bar{\rho}_{vyf} dV = - \int_{\partial V_{iib}} \bar{\rho}_{vyf} (\tilde{w}_j - w_{Gj}) n_j dS + (1 + L_T) \frac{\int_{V_{iib}} \bar{\rho}_{pal} dV}{1-x} \frac{dx}{dt} \quad (19c)$$

$$\int_{V_{iib}} \bar{Q}_V dV = H_u \frac{\int_{V_{iib}} \bar{\rho}_{pal} dV}{1-x} \frac{dx}{dt} \quad (20)$$

The mathematical model was applied to create a Fortran code AMEM3D [15] which deals with modelling of in-cylinder phenomena during compression stroke and expansion stroke of spark ignited (SI) 4-stroke ICE.

3 Computed Cases

A very simple engine geometry was selected to carry out parametric studies to test the mathematical model of ICE. Engine combustion chamber consists of a flat piston and a flat cylinder head – it has the shape of a cylinder. The bore is 85 mm, the stroke 92 mm and the compression ratio is 8. Heat transfer via cooled walls was enabled and specific heat capacity was a function of temperature. Algebraic, one- and two-equation turbulence models (based on Boussinesq hypothesis) were used. Gasoline is used as a fuel. The experimental data [4, 8] were used for comparison with data computed by means of [15]. All the results are presented in [14], the most important results were published in [16–20].

4 Result Discussion

One of the encountered problems was that Reynolds stresses were too small (figures 1-3) when compared with measurement [4] regardless of applied turbulence model, initial

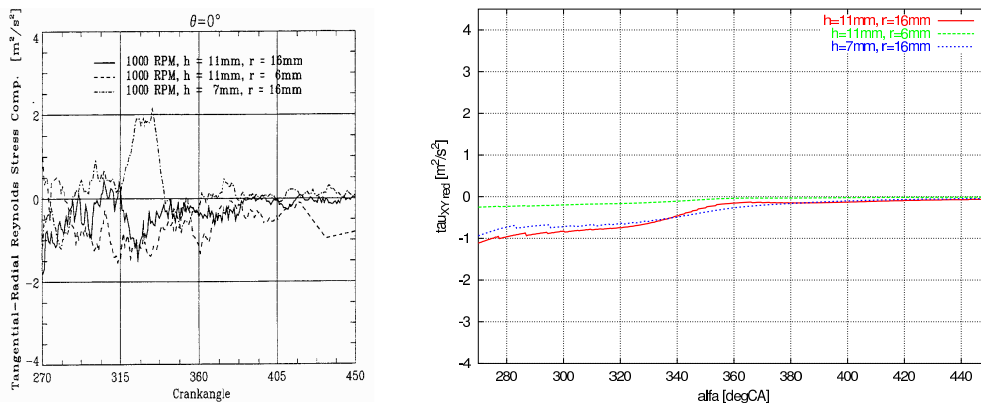


Figure 1: Comparison of corresponding Reynolds stresses (XY component) at three different space locations – measurement data according to [4] (left figure) and computed data (right figure) for the model $1280x35-konv3-k-\tau-VN=5$ at engine speed $n_M = 1000 \text{ min}^{-1}$; data plotted as a function of crank angle (360 degCA corresponds with engine top dead center (TDC)).

conditions or other parameters (numerical solution preciseness, mesh coarseness, etc.). Considering the fact that the engine geometry is very simple, and hence the flow structures are relatively simple as well, it was a negative surprise. On the other hand, it was proven (e.g. [14, 19]) that Boussinesq-type turbulence models applied for the case of ICE have many of the qualitative properties that are known from experience. When comparing predicted and measured integral length scale* (Figure 4), the measurement [8] confirms the assumption that turbulent properties are more or less homogeneous, especially near TDC. The theoretical results basically predicts the same. However, the experimental data suggest that the value of integral length scale is almost symmetrical with respect to TDC. This was not proven by calculations. This is the main qualitative difference – predicted integral length scale is not symmetrical with respect to TDC. If the measured integral length scale is applied for the case of one-equation turbulence model, there is no improvement of predicted Reynolds stress tensor components. Even if algebraic turbulence model is used and very high value of turbulence viscosity is prescribed, the results were not satisfying either. The AMEM3D code was verified against the commercial CFD code [2] to make sure that there is no fundamental problem within the developed algorithm. The main result of this comparison [20] was that the results of both CFD codes are comparable.

It is well known that turbulence properties decrease during compression stroke (unless they are increased by means of combustion chamber shape) and that turbulence generated during intake stroke is dumped at early compression stroke. Moreover, if there are significant differences of properties at the end of intake stroke, there will be much smaller at the end of compression stroke. Generally speaking, this empirical knowledge can be confirmed by computations. Even if different turbulence models are applied, the results satisfy that (Figure 5, right sub-figure) under the assumption that there is significant swirling motion

*The authors are aware of the fact that the exact definition of the turbulence integral length scale is not the same as the value of the length scale which is used in applied turbulence models. However, the authors believe that these two length scales are comparable and their qualitative behavior should be similar. The length scale calculated by applied turbulence models is referenced as predicted integral length scale, even if this is not a precise terminology.

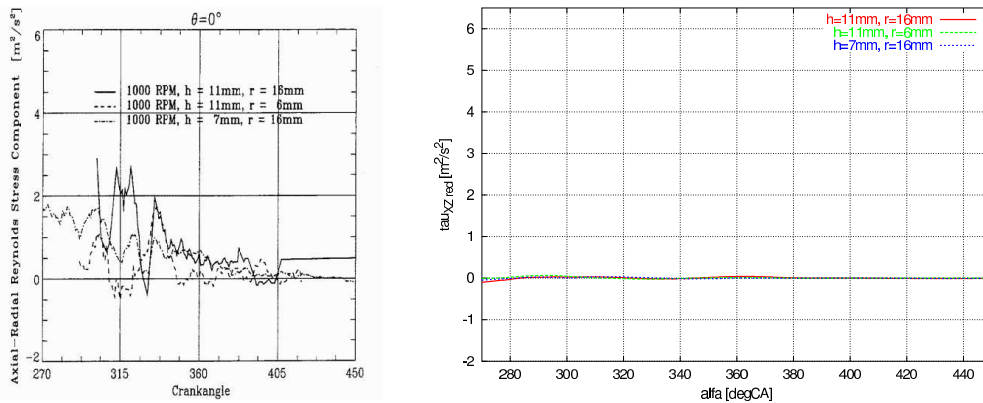


Figure 2: of corresponding Reynolds stresses (XZ component) at three different space locations – measurement data according to [4] (left figure) and computed data (right figure) for the model $1280x35-konv3-k-\tau-VN=5$ at engine speed $n_M = 1000 \text{ min}^{-1}$; data plotted as a function of crank angle (360 degCA corresponds with engine top dead center (TDC)).

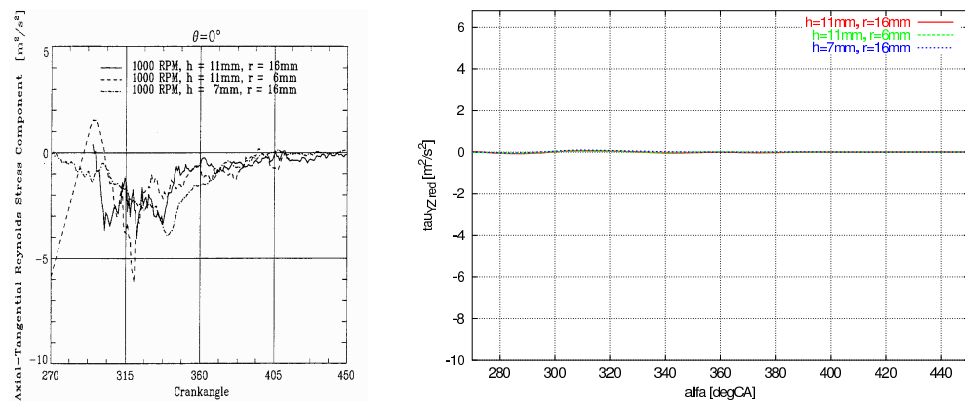


Figure 3: of corresponding Reynolds stresses (YZ component) at three different space locations – measurement data according to [4] (left figure) and computed data (right figure) for the model $1280x35-konv3-k-\tau-VN=5$ at engine speed $n_M = 1000 \text{ min}^{-1}$; data plotted as a function of crank angle (360 degCA corresponds with engine top dead center (TDC)).

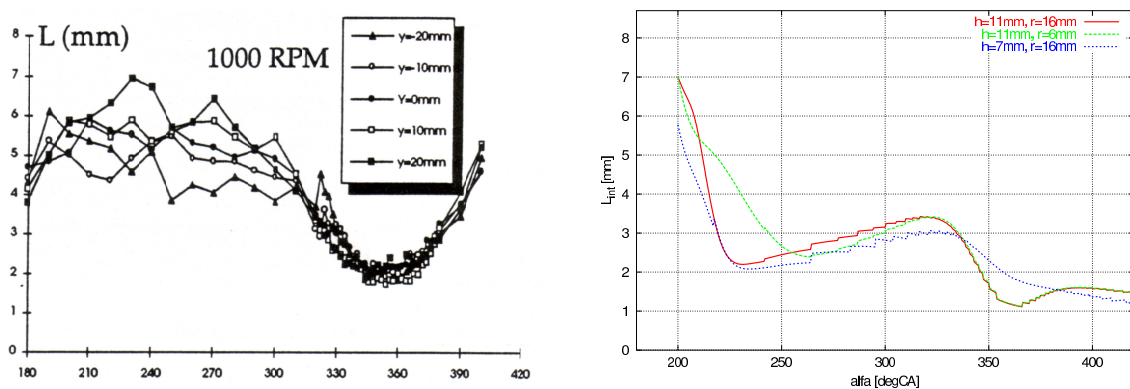


Figure 4: Comparison of integral length scale – measurement data according to [8] (left figure) and computed data (right figure) for the model $1280x35-konv3-k-\tau-VN=5$ at engine speed $n_M = 1000 \text{ min}^{-1}$; data plotted as a function of crank angle (360 degCA corresponds with engine top dead center (TDC)).

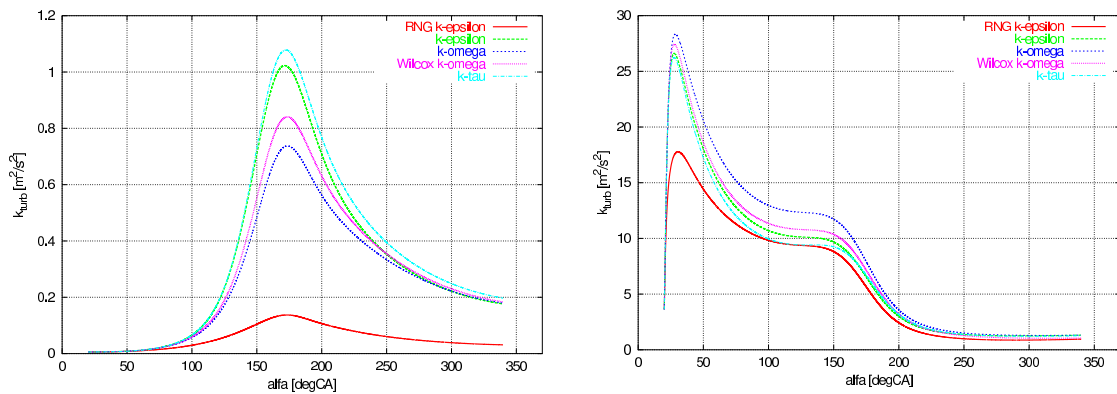


Figure 5: Influence of applied turbulence model for the model 720x25-konv3 at engine speed $n_M = 1000 \text{ min}^{-1}$ – in-cylinder averaged specific turbulence kinetic energy for the case of initial swirl number $VN=0$ (left figure) and initial value of swirl number $VN=5$ (right figure).

at the beginning of compression stroke. On the other hand, if there is no initial swirl and different turbulence models are applied, the results are significantly different (especially *RNG k – ϵ* model). The differences among considered turbulence models become more and more significant. The biggest differences occur at the TDC (Figure 5, left sub-figure). More detailed analysis in [14] suggests that the discussed phenomenon is mainly due to non-linearity of dissipation equation, especially its sink term. It was confirmed that if the considered process is dominated by production of turbulence specific energy k (k increases in time), the dissipation is not adjusted quickly enough – the differences are even more significant during the computation. However, if the process is dominated by dissipation of k (k is decreased in time), all models predict almost the same results.

Regarding application of simple combustion model based on the *Level Set* approach, there are two issues. Firstly, the model should be suitable for SI engine combustion modelling as the mixture is already well mixed and turbulent transport is the dominant phenomenon – this statement is valid if temperatures are high enough which is the case when engine load is high. Taking into account this fact, it is a bit surprising that the shape of ROHR is relatively different when compared with experimentally measured one (Figure 6). Moreover, the ROHR shape cannot be changed by means of tuning the model constants. However, the predicted shape of ROHR seems to be in a good correspondence with modelled processes. The combustion itself is a significant source of turbulence which causes that turbulent flame speed is increased. This leads to even faster flame front propagation which causes that more energy is released per unit time. Another important fact is that as the combustion proceeds in time, the unburnt mixture is compressed (density is higher). These two phenomena clearly must cause that the ROHR is more significant at the end of combustion process. The only fact which may change the shape of calculated ROHR is the chemical dissociation (not taken into account in presented results; more details can be found in [22]) – it can work as a capacitor which stores the energy at very high temperatures and once the temperature decreases, the energy is released back. There seems to be no other reason that combustion speed should be decreased at the end of combustion process if turbulent transport is the dominant factor. Secondly, it was proven that combustion model constants should be tuned in such a way that they compensate for the influence of both applied turbulence model and mesh coarseness. Especially the latter phenomenon is very

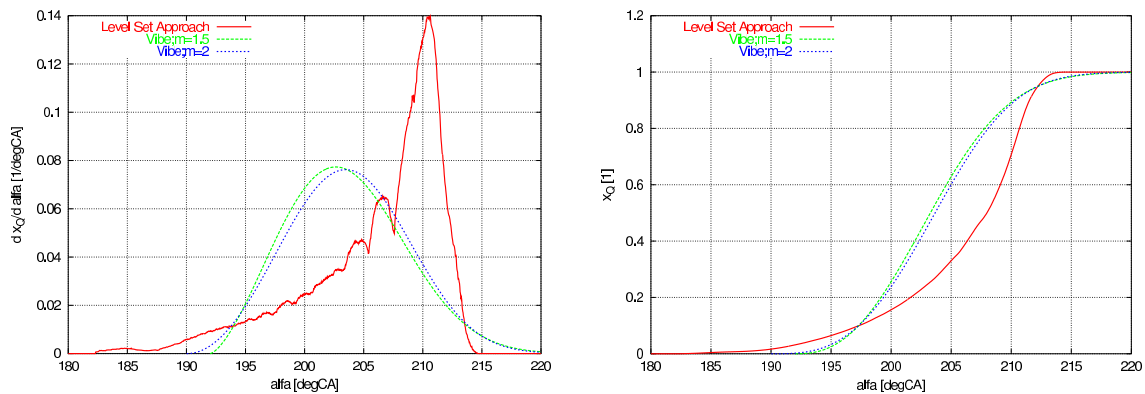


Figure 6: Comparison of computed ROHR (*Level Set* approach) with typical experimental curve of ROHR (Vibe exponent in the range from 1.5 to 2.0) – differential form of ROHR (left figure) and integral form of ROHR (right figure) .

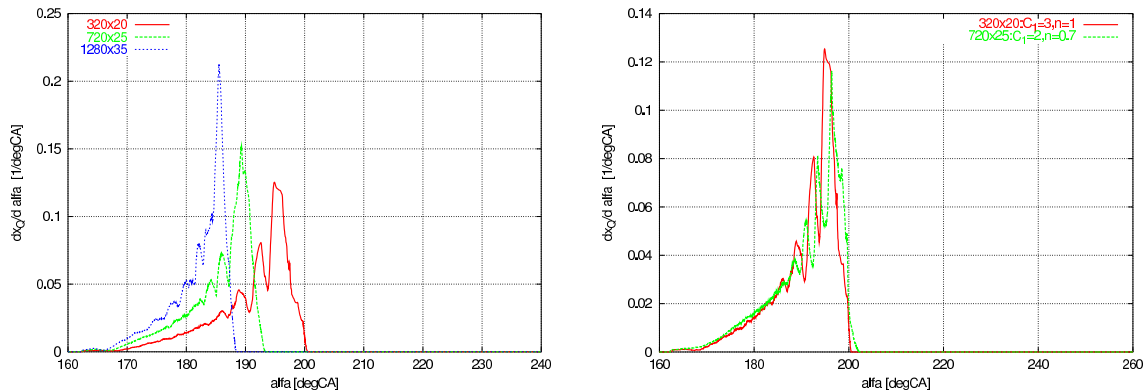


Figure 7: Influence of mesh on ROHR for the model *konv3-k- τ -HEAT-REAL_GAS-G_function* at engine speed $n_M = 5000 \text{ min}^{-1}$ – the same value of combustion model calibrating constants applied for all meshes (left figure) and different value of calibrating constants for each mesh to keep the same flame front propagation speed (right figure).

significant (Figure 7, left sub-figure). This corresponds well with the already mentioned facts concerning turbulence flame speed and dissipation equation – the finer mesh causes that velocity gradients are smeared less. This causes higher source term of k , dissipation model is not fast enough to take some correction action.

5 Conclusion

The presented contribution deals with significant problems of Boussinesq-type turbulence model application in ICE. It should be stressed that two-equation turbulence models are routinely used when performing multi-dimensional simulations in ICEs. The presented data and encountered problems were obtained when working on [14]. The paper main target was to stress the important problems of turbulence modelling in ICE.

It seems that Reynolds stress quantitative prediction is important weak point of the considered approach. If turbulent momentum transport cannot be trusted, temperature turbulent transport is most likely wrong as well. This conclusion might cast doubts over chemical-kinetics-based simulations for which the proper temperature prediction is very

important. Moreover, it seems that different turbulence models vary significantly in modeling of dissipation. This causes that the results might be very different. On the other hand, it should be mentioned that two-equation turbulence models have such properties that qualitative influence of many phenomena is in a good correspondence with experimental knowledge (detailed description is presented in [14, 19]).

Simple combustion model based on assumption that turbulent transport is the dominant term (which should be valid for SI engine under high engine load) has many positive properties (more details can be found in [14]). However, the shape of ROHR and significant influence of applied mesh are the most important weak points.

Many hopes are put in the *Large Eddy Simulation* (LES) techniques (e.g. [7]). Some promising results have been obtained using this approach – e.g. [3, 6, 9, 12]. However, the authors are a bit sceptic about it. The LES approach should prove first that progress can be made for proper modelling of momentum and energy transport in ICE. After that, additional effort for developing advanced models for other phenomena (combustion, pollutant production, cycle variability, etc.) might be important.

Acknowledgement

This work has been supported within the MŠM project Z20760514 "Komplexní dynamické systémy v termodynamice, mechanice tekutin a těles". This help is gratefully appreciated.

References

- [1] *Fire 8.2 for Windows [CD-ROM]*. AVL List GmbH, 2003.
- [2] *Fluent 6.1 Documentation [CD-ROM]*. Fluent Inc., February 2003.
- [3] Celik, I., Yavuz, I., and Smirnov, A. *Large Eddy Simulations of In-cylinder Turbulence for Internal Combustion Engines: a Review*. *International Journal of Engine Research*, Vol. 2(2):119–148, 2001. ISSN 1468-0874.
- [4] Dimopoulos, P. and Boulouchos, K. *Reynolds Stress Components in the Flow Field of a Motored Reciprocating Engine*. *SAE Technical Paper Series*, March 1995. Paper 950725.
- [5] Dvořák, R. and Kozel, K. *Matematické modelování v aerodynamice*. Lecture notes of CTU. CTU in Prague, Prague, 1996. ISBN 80-01-01541-6. (In Czech).
- [6] Haworth, D. C. *Large Eddy Simulations of In-cylinder Flows*. *Oil and Gas Sci. Technol. Rev., IFP*, Vol. 54(2):175–185, 1999.
- [7] Lesieur, M., Métails, O., and Comte, P. *Large-Eddy Simulations of Turbulence*. Cambridge University Press, 40 West 20th Street, New York, NY 10011-4211, USA, 2005. ISBN 0-521-78124-8.

- [8] Michard, M., Lengyel, I., and Grosjean, N. *Measurements of Turbulence Length Scales in a Motored Reciprocating Engine. In: 2nd International Symposium on Experimental and Computational Aerothermodynamics of Internal Flows – Proceedings*, Vol. 2:381–386, July 1993.
- [9] Naitoh, K., Itoh, T., and Takagi, Y. *Large Eddy Simulations of Premixed Flame in Engine Based on the Multilevel Formulation and the Renormalization Group Theory. SAE Technical Paper Series*, February 1992. Paper 920590.
- [10] Peters, N. *Turbulent Combustion*. The Press Syndicate of the University of Cambridge, The Pitt Building, Trumpington Street, Cambridge, 2000. ISBN 0-521-66082-3.
- [11] Sethian, F. A. *Level Set Methods*. Cambridge Monographs on Applied Computational Mathematics. Cambridge University Press, Cambridge, U.K., 1996.
- [12] Smirnov, A., Yavuz, I., and Celik, I. *Diesel Combustion and LES of In-Cylinder Turbulence for IC-Engines. In: ASME Fall Technical Conference on In-Cylinder Flows and Combustion Processes, Ann Arbor, Michigan*, pages 119–127, 1999. Paper 99-ICE-247.
- [13] Swanson, R. C. and Turkel, E. *Multistage Schemes with Multigrid for Euler and Navier-Stokes Equations*. NASA Technical Paper 3631, NASA, 800 Elkridge Landing Road, Linthicum Heights, MD 21090-2934, August 1997.
- [14] Vítek, O. *Simulace dějů v pístovém motoru s vlivem turbulence*. Ph.D. Thesis, CTU in Prague, Department of Automotive Engineering, 2006. (In Czech).
- [15] Vítek, O. and Polášek, M. *AMEM3D: CFD Program for Modelling of In-cylinder Phenomena*, 2004-2005. Program Library – Ú 220.
- [16] Vítek, O., Polášek, M., Kozel, K., and Macek, J. *First Approach to Combustion Modeling in an SI Engine. In: Topical Problems of Fluid Mechanics 2004, Prague*, pages 15–16, February 2004. ISBN 80-85918-86-2.
- [17] Vítek, O., Polášek, M., Kozel, K., and Macek, J. *Premixed Turbulent Combustion Modeling Using Level Set Approach. GAMM 2005 Abstracts*, Vol. 1:182, March 2005.
- [18] Vítek, O., Polášek, M., Kozel, K., and Macek, J. *U-RANS Model of Internal Combustion Engine. Proceedings: Symposium on Hybrid RANS-LES Methods*, page 17, July 2005.
- [19] Vítek, O., Polášek, M., Kozel, K., and Macek, J. *Linear Turbulence Model Validation for the Case of 3-D In-cylinder Phenomena Modeling. Journal of Middle European Construction and Design of Cars (MECCA)*, Volume V. (04/2006 + 01/2007):24, 2007. ISSN 1214-0821.

- [20] Vítek, O., Polášek, M., and Mareš, B. *Proudění ve spalovacím motoru během vysokotlaké části oběhu*. In: *Sborník přednášek KoKa 2004, Brno*, pages 138–143, September 2004. (In Czech), ISBN 80-7157-776-6.
- [21] Wilcox, D. C. *Turbulence Modeling for CFD*. DCW Industries, Inc., 5354 Palm Drive, La Canada, California 91011, 2. edition, March 2000. ISBN 0-9636051-5-1.
- [22] Zacharias, F. *Mollier-I,S-Diagramme für Verbrennungsgase in der Datenverarbeitung*. *Motortechnischezeitschrift (MTZ)*, 31(7):296–303, 1970.